



CALIBRATION OF A LASER-DOPPLER ANEMOMETER BY MEANS OF CALIBRATION DISK

Fábio Ouverney Costa

Felipe dos Santos Ferreira

National Institute of Metrology, Quality and Technology – Inmetro
Directory of Scientific and Industrial Metrology – Dimci
Fluid Dynamics Metrology Division – Dinam
Av. Nossa Senhora das Graças, 50 Prédio 6, Duque de Caxias - RJ
fsferreira@inmetro.gov.br

José Luiz Zanon Zotin

National Institute of Metrology, Quality and Technology – Inmetro
Directory of Scientific and Industrial Metrology – Dimci
Fluid Dynamics Metrology Division – Dinam
Av. Nossa Senhora das Graças, 50 Prédio 6, Duque de Caxias - RJ
jlzotin@gmail.com

Maurício Nagl

National Institute of Metrology, Quality and Technology – Inmetro
Directory of Scientific and Industrial Metrology – Dimci
Fluid Dynamics Metrology Division – Dinam
Av. Nossa Senhora das Graças, 50 Prédio 6, Duque de Caxias - RJ
mauricio.nagl@hotmail.com

Samuel Araújo

National Institute of Metrology, Quality and Technology – Inmetro
Directory of Scientific and Industrial Metrology – Dimci
Fluid Dynamics Metrology Division – Dinam
Av. Nossa Senhora das Graças, 50 Prédio 6, Duque de Caxias - RJ
saraujo@inmetro.gov.br

Valter Yoshihiko Aibe

National Institute of Metrology, Quality and Technology – Inmetro
Directory of Scientific and Industrial Metrology – Dimci
Fluid Dynamics Metrology Division – Dinam
Av. Nossa Senhora das Graças, 50 Prédio 6, Duque de Caxias - RJ
vyaibe@inmetro.gov.br

Abstract. *This work presents the method used by Inmetro for the calibration of a Laser-Doppler anemometer. The calibration is carried out using a calibration disk with constant angular velocity, as a primary standard. Thus, the calibration is done by direct comparison between the velocities given by the instrument with the tangential velocity of the calibration disk.*

Keywords: LDA, Calibration, Anemometry

1. INTRODUCTION

With the advance of optical technology and electronic processing, the Laser-Doppler Anemometry (LDA) has become a robust technique. This technique utilizes the Doppler Effect for evaluating the fluid velocity at a given point of the flow. A light source is used to generate two beams that intersect, giving rise to interference fringes. The region of intersection of two beams, where the flow is actually measured, is called intersection volume. Small particles in the fluid that pass through the intersection volume cause light scattering, which is detected by an optical system and sent to a signal processor. The frequency of the scattered light is directly proportional to the particle velocity, which is assumed to be equal to the fluid velocity component that is in the plane perpendicular to the interference fringes (Albrecht, et al., 2003; Freire, et al., 2006; Zhang, 2010).

The Doppler effect occurs when the transmitter (or receiver) of an electromagnetic wave is moving, resulting in a variation of the frequency and wavelength in respect to the originally emitted wave. This frequency range is known as the Doppler shift.

“Equation (1)” shows how the LDA calculate the speed.

F. O. Costa, F. S. Ferreira, J. L. Z. Zotin, M. Nagl, S. Araújo and V. Y. Aibe
Calibration Of A Laser-Doppler Anemometer By Means Of Calibration Disk.

$$V = \delta \cdot f_{doppler} . \quad (1)$$

The distance between two successive fringes (δ) depends only on the wavelength of the laser (λ) and the angle of intersection (θ) as shown in “Eq. 2” and illustrated in “Fig. 1”.

$$\delta = \frac{\lambda}{2 \sin\left(\frac{\theta}{2}\right)} . \quad (2)$$

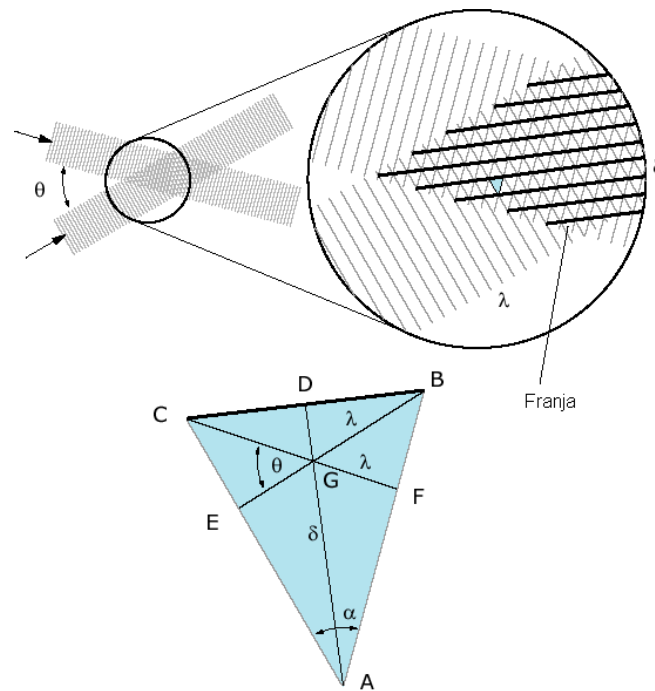


Figure 1. Fringe space calculation (Efunda,2013).

A frequently used method to calibrate a LDA is the rotating disk method. The rotating disk is the velocity primary standard. In this case, the LDA is calibrated directly on terms of velocity. One of the methods uses a rotating sandpaper disk and was used by Park, et al. (2002). A second method uses a rotating wire and was applied by National Institute of Standards and Technology (NIST) and by National Metrology Institute of Japan (NMIJ). Both used a tungsten wire. The difference between this method and the previous one is that in the first one the irregularities works as many particles passing simultaneously through the intersection volume, and in the second one the wire works as a single well defined particle. A third method uses a glass disk and was used by Lu, et al. (2001) from Physikalisch-Technische Bundesanstalt (PTB). In this case, the velocity is measured at the cylindrical surface normal to the axis of rotation rather than on the surface for sandpaper disk. But, as the sandpaper disk, the rotating glass disk also measures multiple particles per revolution (ITTC, 2008).

For calibration of LDA, we used the system of velocity standardization deployed by Fluid Dynamics Metrology Division. This system consists of a rotating disk, a tachometer, a data acquisition and signal processing board, a host computer and a positioning system.

The rotating disk has some roughness on its surface. Such irregularities will act as particles mixed into the fluid during the experiments. Therefore, the disk was positioned so that the LDA makes the measurement of the velocity of such irregularities, which means, the measurement of the tangential velocity of the disk. The disk has a constant angular velocity. Therefore, it's possible to calculate the tangential velocity of the disk starting with the following formula:

$$V = \omega \times R , \quad (3)$$

where V is the tangential velocity, ω the angular velocity and R is the radius of the disk.

Finally, the calibration of the LDA was made by direct comparison between the velocity indicated by the LDA and the calibrated velocity of the standardization system.

2. DEVELOPMENT

To ensure that the intersection volume is positioned on the surface of the disk (“Fig. 2”), it was used a positioning system with three axes (*Sigma Koki SGSP 46-500* with 0.025 mm of accuracy), as shown in “Fig. 3”.

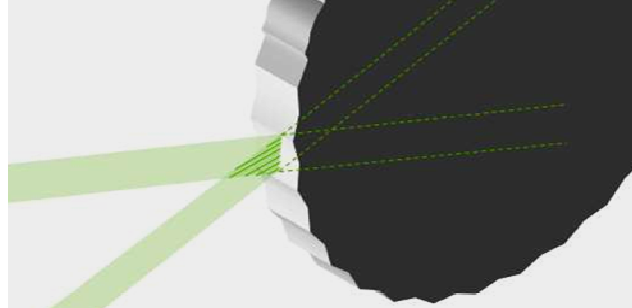


Figure 2. Intersection volume positioned on the disk surface.

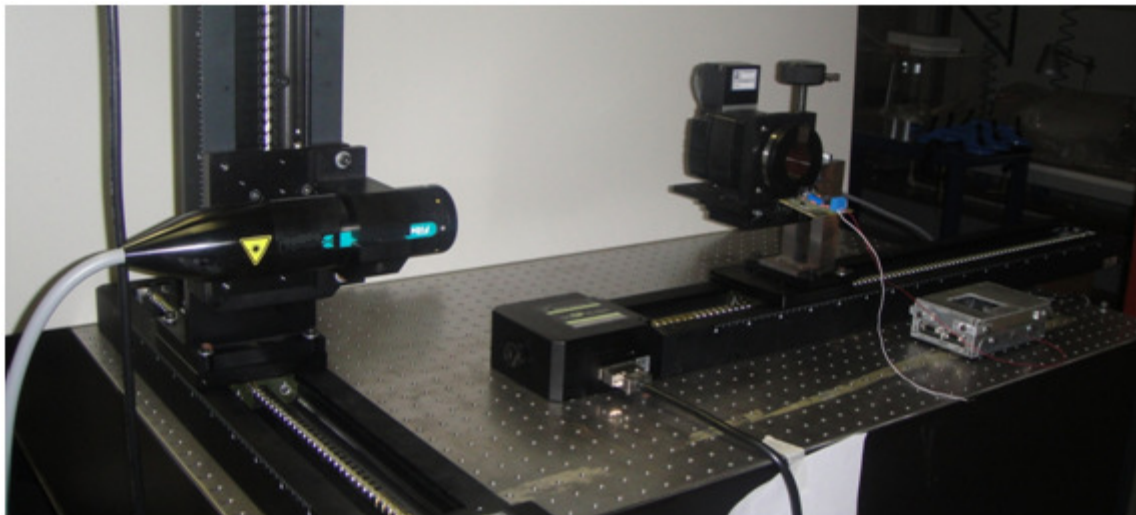


Figure 3. Positioning system with three axes. Two axes were dedicated to LDA probe (left side) and one to calibration disk (right side).

The disk has a constant angular velocity. An optical tachometer monitors the duration of each revolution of the disk to determine the angular frequency uncertainty. The reference time-base clock of velocity primary standard system was verified by the Laboratory of Optical Communications, Radio-Frequency and Time and Frequency of INMETRO. The disk diameter was calibrated by Dimensional Metrology Laboratory of INMETRO. Then, it could be secured a calibrated and traceable linear velocity.

3. SOURCES OF UNCERTAINTY

3.1 Disk

3.1.1 Diameter

The measuring surface of the disk was calibrated on the diameter. The calibration certificate supplied deviation values of diameter in two orthogonal pairs of points and out-of-roundness. The uncertainty disk diameter is much smaller than the out-of-roundness. Then, the uncertainty in diameter was considered only as the out-of-roundness in the range used (Tab. 1 and Tab. 2).

Table 1. Results of measurements of the diameters

D1	U	D2	U
(mm)	(μm)	(mm)	(μm)

F. O. Costa, F. S. Ferreira, J. L. Z. Zotin, M. Nagl, S. Araújo and V. Y. Aibe
Calibration Of A Laser-Doppler Anemometer By Means Of Calibration Disk.

80,0962	0,6	80,1158	0,6
---------	-----	---------	-----

Table 2. Results of measurements of the deviations from circularity

Circularity Deviations	U
(mm)	(μm)
0,0214	0,5

3.1.2 Tachometer Clock

The tachometer was verified as to the frequency of its reference clock. The value clock uncertainty value is 0.2 Hz and the uncertainty of the number of clock pulses was ± 1 .

3.1.3 Angular Velocity

During the measurement, the period of each turn of the calibration disk was monitored, and its standard deviation was considered as the uncertainty of the angular velocity.

3.1.4 Thermal Expansion

Due to the lack of information about the thermal expansion of the disk material, it was used a mean value for stainless steel with an estimated uncertainty of 20%.

3.1.5 Other Sources of Errors

Effects of elastic deformation due to the inertia of the disk will be disregarded. The center of rotation is taken as the same center passed by the diameters calibrated. Effects of vibration can be ignored due to the action of anti-vibration table.

3.2 LDA

3.2.1 Distance Between Fringes

It is important that the measurements with the laser Doppler system are carried out with the intersection volume aligned at the both beam waists, because in this beams region, the electromagnetic wave fronts may be considered flat. Moreover, when the intersection occurs outside beams waist, the wave fronts have a certain curvature, resulting in a non-constant spacing of the interference fringes, that is, the distance between fringes becomes dependent on their position within the intersection volume as shown in "Fig. 4" (Zhang, 2010). Consequently, the measured Doppler frequency is also dependent on the position of the particle in the intersection volume and no longer linearly proportional to the fluid velocity.

The intersection of the beams in an improper location results in distortion of the surface of the fringes and the lack of parallelism between the planes. Under this condition, particles of the same speed cross the intersection volume in different places producing different Doppler frequencies, masking the correct speed value.

The asymmetric geometry of the intersection volume can be measured, in this case, by the photomultiplier anode current value. This parameter depends on the particle concentration and the sensitivity of the optical LDA system. The sensitivity was maintained constant during experiments. So, the photomultiplier anode current value can be considered proportional to the light intensity inside the intersection volume. It is known that the light intensity distribution in the cross section of an intersection volume can be represented by Gaussian distribution (Zhang, 2010), with its maximum at the intersection volume center. "Figure 5" shows the experiments results obtained for the photomultiplier anode current. As it can be seen, the distribution is not symmetric along the intersection volume, which indicates an incorrectly aligned system as shown in "Fig 4".

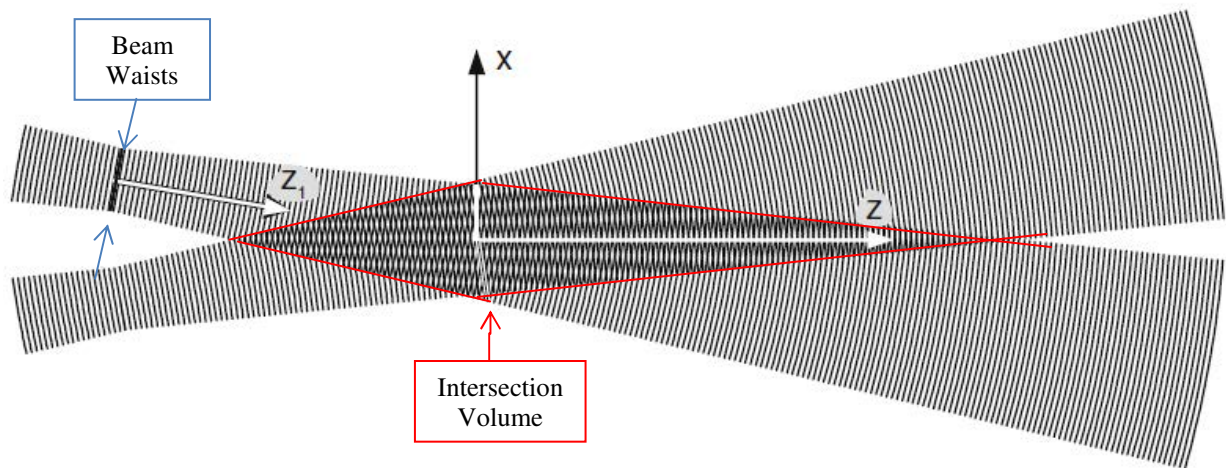


Figure 4. Fringe spacing variation in an incorrectly aligned system (Zhang, 2010).

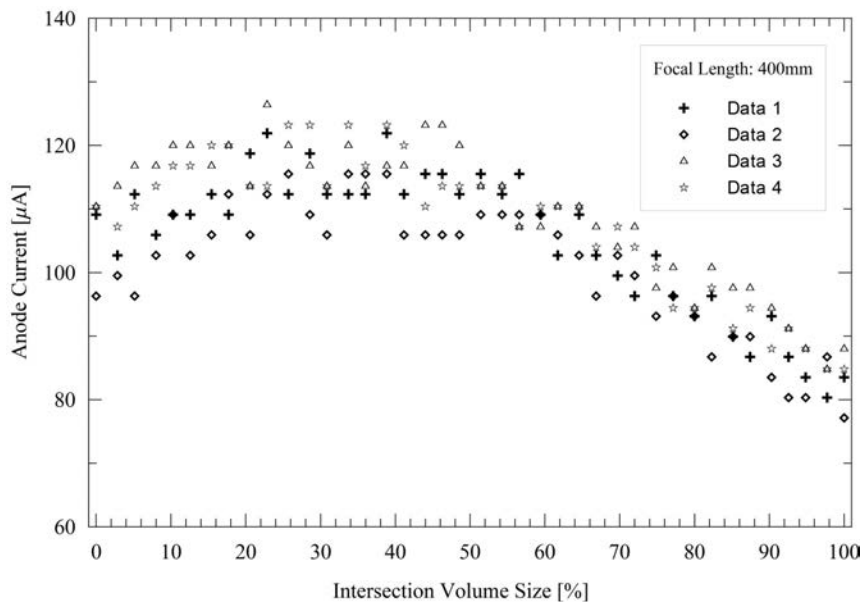


Figure 5. Photomultiplier anode current measured along the intersection volume.

3.2.2 Probe Thermal Expansion

Variations in temperature probe also cause variations in the location of the intersection of the beams, causing distortions in the interference fringes. This effect was disregarded in modeling and entered in the random speed variation displayed by LDA (δV_{LDA}).

3.2.3 Burst Frequency Calculation

Errors concerning the frequency calculation by the Burst Spectrum Analyzer (BSA) entered in the random speed variation displayed by LDA (δV_{LDA}).

3.2.4 Other Source of Errors

The uncertainty of the wavelength of the laser beam was disregarded.

3.3 System Alignment

In order to guarantee the correct reading of the disk tangential velocity, the horizontal axis of the laser beams intersection volume must be aligned with the center of the disk ("Fig. 6.b"). Otherwise, the LDA will measure a smaller component value of tangential velocity ("Fig. 6.a").

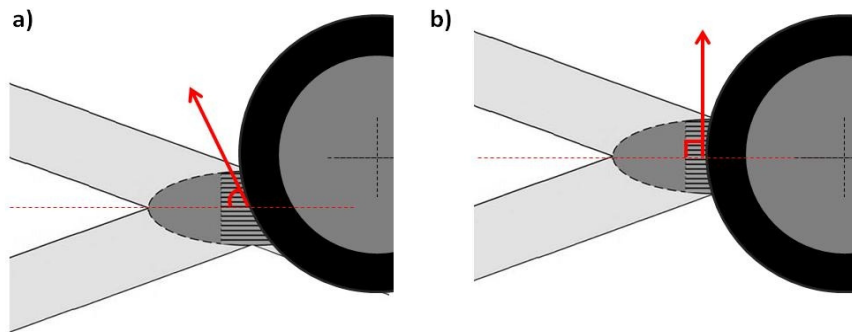


Figure 6. Correct alignment between the disk and the intersection volume.

4. MATHEMATICAL MODELING

The calibration factor was calculated by directly comparing the linear velocity reference, calibrated and traceable, with the speed provided by the LDA:

$$C = \frac{V_r}{V_{LDA}} = \frac{\omega_D R}{V_{LDA}} = \frac{\pi f_D D}{V_{LDA}} = \frac{\pi D}{T \cdot V_{LDA}} .$$

The calculation of the disk period was made based on the number of clock pulses counted by the tachometer. This way:

$$n_p = f_c T_d \rightarrow T_d = \frac{n_p}{f_c} .$$

4.1 Fringes Spacing Variation Along the Interference Volume

As the interference fringes are not parallel throughout all the interference volume is to be expected that the value obtained at each point is different. The chart below (“Fig. 7”) shows the results of the speed provided by the LDA in various parts of the intersection volume:

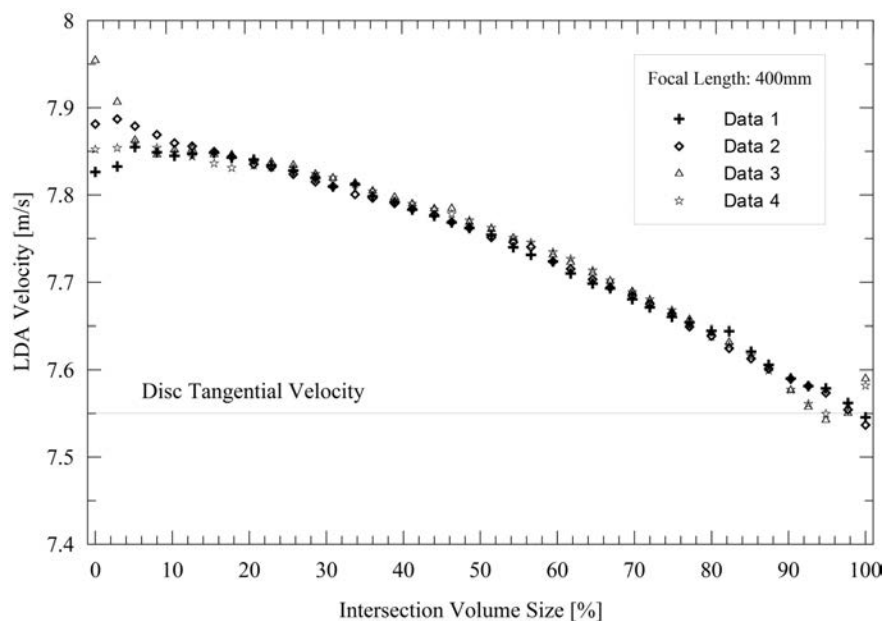


Figure 7. – Tangential velocity measured with LDA.

In this way, it is necessary to calibrate several points of the interference volume.

However, although it can be assumed that the intersection volume has a uniform particles distribution, the probability of LDA to detect the motion of a particle is not constant over its entire length. The image below demonstrates this feature:

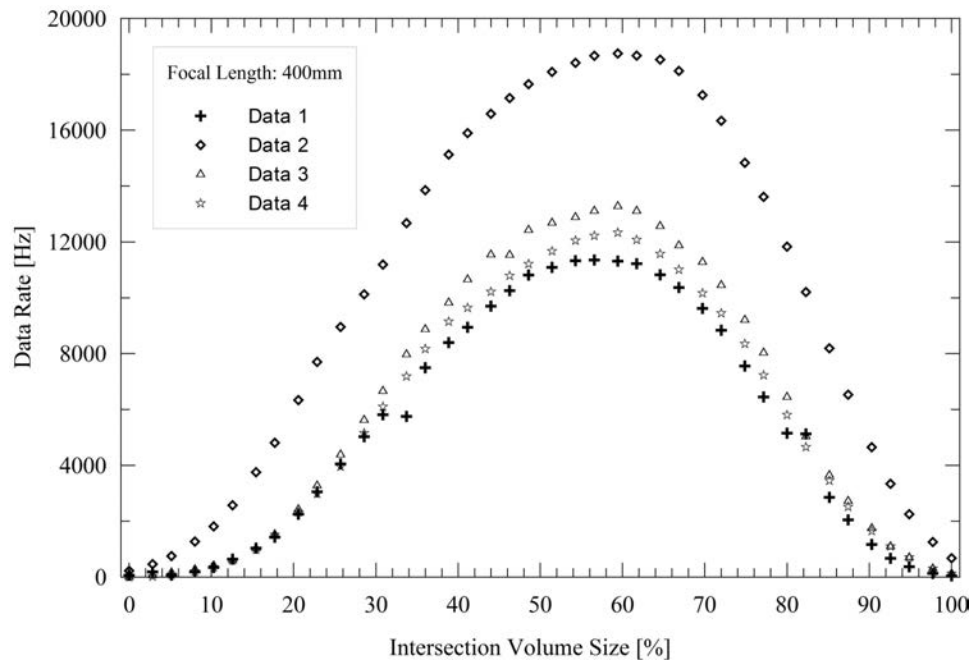


Figure 8. Data rate obtained for each point measured.

The data rate (quantity of speed values considered by the LDA per second) varies depending on the position of the particle in the interference volume ("Fig. 8"). It is evident that the probability of a particle to be detected is greater at the center than at the edges.

Therefore, it is necessary to calculate a weighted average using the data rate. One way to do this is to set the sampling time and use all captured data by the LDA in several points of the interference volume to obtain an average and a standard deviation:

$$V_{LDA} = \frac{\sum_{i=1}^n \sum_{j=1}^{m_i} V_{ij}}{\sum_{i=1}^n m_i} ,$$

$$\delta V_{LDA} = \sqrt{\frac{1}{\sum_{i=1}^n m_i} \sum_{i=1}^n \sum_{j=1}^{m_i} (V_{ij} - \bar{V}_{LDA})^2} ,$$

where n is the number of points in the interference volume and m_i is the amount of the values detected by the LDA in the i -th position of the intersection volume.

4.2 Misalignment correction of the Laser Beam Plane in comparison to the calibration disk plane :

To find just the projection perpendicular to the interference fringes of the velocity vector, it is necessary to correct the misalignment between the laser and the disk calibration. Let θ_y be the rotation about the y-axis, θ_x the rotation about the x-axis and h the vertical distance between the intersection volume and disk rotation axis, the real velocity measured by LDA will be given by the expression:

$$V'_d = V_d \cos \varphi \cos \theta_y ,$$

where

$$\varphi = \theta_x + \sin^{-1} (2h/D) ,$$

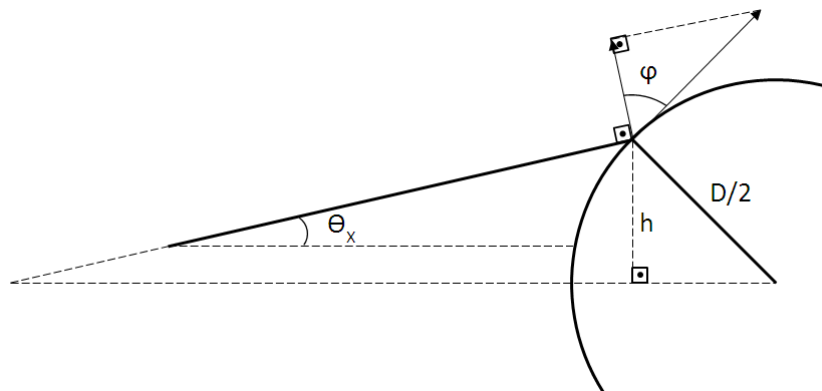


Figura 9 - Misalignment correction of the Laser Beam Plane.

4.3 Correction of the diameter by the temperature variation.

The thermal expansion of the disk was given by:

$$D = D_0(1 + \alpha(T_m - T_r)) ,$$

where D_0 is the calibrated diameter, α is the linear thermal expansion coefficient, T_m is the temperature measured during the experiments and T_r is the reference temperature. The air temperature were measured near the disk during all experiment with a digital baro-thermo-hygro sensor (BTHR918N – Oregon Scientific) calibrated at Inmetro.

4.4 Full Mathematical Model:

Finally the full mathematical model can be represented as:

$$C_k = \frac{\pi D_0 \left(1 + \alpha((T_m + \delta T_m) - T_r)\right) \cos\left(\theta_x + \sin^{-1}\left(\frac{2h}{D}\right)\right) \cos(\theta_y)}{\left(\frac{\bar{n}_p + \delta n_p}{f_c}\right) (\bar{V}_{LDA} + \delta V)} ,$$

where C_k is the calibration factor with uncertainty for a particle moving in an unknown point of the intersection volume, δT_m , δn_p and δV are random variations of temperature, the number of clock pulses read by the tachometer and the velocity obtained by LDA during the measurements, respectively.

To calculate the correction and uncertainty of the mean velocity in the control volume:

$$C = \bar{C} + \delta C ,$$

where δC is the standard deviation of C and \bar{C} is the mean of the l measurement groups:

$$\bar{C} = \sum_{k=1}^l \frac{C_k}{k} .$$

4.5 Uncertainty Calculation

The uncertainty calculation was done according to the 3rd edition of the Brazilian "Guide to the Expression of Uncertainty in Measurement" (ISO-GUM).

Let Y be the mathematical model of a function of N variables:

$$Y = f(x_1, x_2, \dots, x_N) .$$

The combined standard uncertainty $u_c(y)$, where y is the estimate of the measurand Y , is given by:

$$u_c^2(y) = \sum_{i=1}^N \left[\frac{\partial f}{\partial x_i} \right]^2 u^2(x_i) ,$$

where $u(x_i)$ is the standard uncertainty of the i -th variable.

4.6 Results

For the calibration, 5 groups of measurements with acquisition time of 30s each point and 14 equidistant points inside the intersection volume were made.

Table 1. LDA Calibration results for a particle passing through out an unknown point of the intersection volume (C_k).

Mean		0.975
Expanded Uncertainty		0.0149
Combined Uncertainty		0.00748
Coverage Factor		1.999
Relative Expanded Uncertainty		1.534 %
Contributions	D_0	1.01%
	α	$3.12 \times 10^{-2} \%$
	tmed	$3.62 \times 10^{-2} \%$
	δt_{med}	$3.72 \times 10^{-3} \%$
	tr	$3.63 \times 10^{-2} \%$
	θ_x	$2.77 \times 10^{-1} \%$
	θ_y	$2.77 \times 10^{-1} \%$
	np	$1.45 \times 10^{-2} \%$
	δnp	1.51 %
	fc	$4.21 \times 10^{-5} \%$
	Vm	$4.71 \times 10^{-7} \%$
δVm	96.80%	

5. CONCLUSIONS

With the LDA system calibrated, it is possible to perform calibrations of other anemometric systems in a wind tunnel, using the LDA as standard. Thus, the velocity reference is given by:

$$V_{corr} = C V_{LDA} ,$$

where C was calculated with a mean value of 0.975 and a uncertainty of 0,0149 (1.53%) for a confidence interval of 95%, ie $k = 2$.

It is important to note that the calibration is valid for a specific system, with all components and settings kept constant. Thus, to ensure a calibration factor with the same mean value and uncertainty, measures should be carried out in flows with low turbulence, around 7.55m/s, and with the same optical system and assembly.

Smaller uncertainties can be obtained by improving the alignment of the lasers beams, so that both of them intersect at theirs waist and using a system (rotating wire), where only one burst signal is detected every time. These systems allow uncertainties below 1% and are used in several institutes metrology.

Future work will be done to improve the mathematical modeling, to include sources of uncertainty not considered in this work, as well as improve the simulation of a real flow.

The rotating disk system will also be changed for operation in other rotation frequency, allowing calibration at a higher range of velocity.

6. REFERENCE

Albrecht, H.-E., Borys, M., Damaschke, N. and Tropea, C., 2003. "Laser Doppler and Phase Doppler Measurement Techniques", Springer.

F. O. Costa, F. S. Ferreira, J. L. Z. Zotin, M. Nagl, S. Araújo and V. Y. Aibe
Calibration Of A Laser-Doppler Anemometer By Means Of Calibration Disk.

Efunda, 2013. "Interference of Two Plane Waves". 30 May. 2013 <http://www.efunda.com/designstandards/sensors/laser_doppler/laser_doppler_flow_theory.cfm>.

Freire, A. P. S., Ilha, A. and Colaço, M. J., 2006. "Turbulência", Associação Brasileira de Ciências e Engenharia Mecânica (ABCM).

ITTC, 2008. "Uncertainty Analysis: Instrument Calibration", ITTC Recommended Procedures and Guidelines 7.5-01-03-02.'

Lu, J., Mickan, B., Shu, W., Kurihara, N. and Dopheide, d., 2001. "Research of the LDA Calibration Facility's Uncertainty", Physikalisch-Technisch Bundesanstalt (PTB), Germany.

Park, J. T., Cutbirth, J. M. and Brewer, W. H., 2002. "Hydrodynamic Performance of the Large Cavitation Channel (LCC)", Technical report NSWCCD-50-TR- 2002/068, Naval surface Warfare Center Carderock Division, West Bethesda, Maryland USA.

Yeh, T.T. and Hall J.M., "Airspeed Calibration Service" - NIST Special Publication 250-79.

Zhang, Zh., 2010. "LDA Application Methods – Laser Doppler Anemometry for Fluid Dynamics", Springer.

7. RESPONSIBILITY NOTICE

The author(s) is (are) the only responsible for the printed material included in this paper.